

AEDC-TR-81-11

DOC NUM SER CN
UNC10965-PDC A 1



Use of the Pitot Tube in Very Low Density Flows

W. B. Stephenson
Calspan Field Services, Inc.

October 1981

Final Report for Period February 1964 — January 1981

Approved for public release; distribution unlimited.

**ARNOLD ENGINEERING DEVELOPMENT CENTER
ARNOLD AIR FORCE STATION, TENNESSEE
AIR FORCE SYSTEMS COMMAND
UNITED STATES AIR FORCE**



NOTICES

When U. S. Government drawings, specifications, or other data are used for any purpose other than a definitely related Government procurement operation, the Government thereby incurs no responsibility nor any obligation whatsoever, and the fact that the Government may have formulated, furnished, or in any way supplied the said drawings, specifications, or other data, is not to be regarded by implication or otherwise, or in any manner licensing the holder or any other person or corporation, or conveying any rights or permission to manufacture, use, or sell any patented invention that may in any way be related thereto.

Qualified users may obtain copies of this report from the Defense Technical Information Center.

References to named commercial products in this report are not to be considered in any sense as an indorsement of the product by the United States Air Force or the Government.

This report has been reviewed by the Office of Public Affairs (PA) and is releasable to the National Technical Information Service (NTIS). At NTIS, it will be available to the general public, including foreign nations.

APPROVAL STATEMENT

This report has been reviewed and approved.



ELTON R. THOMPSON
Director, Project Analysis and Engineering
Deputy for Operations

Approved for publication:

FOR THE COMMANDER



JOHN M. RAMPY
Director of Aerospace Flight Dynamics Test
Deputy for Operations

UNCLASSIFIED

| REPORT DOCUMENTATION PAGE | | READ INSTRUCTIONS BEFORE COMPLETING FORM |
|--|-----------------------|---|
| 1. REPORT NUMBER AEDC-TR-81-11 | 2. GOVT ACCESSION NO. | 3. RECIPIENT'S CATALOG NUMBER |
| 4. TITLE (and Subtitle) USE OF THE PITOT TUBE IN VERY LOW DENSITY FLOWS | | 5. TYPE OF REPORT & PERIOD COVERED Final Report - February 1964 - January 1981 |
| | | 6. PERFORMING ORG. REPORT NUMBER |
| 7. AUTHOR(s) W. B. Stephenson, Calspan Field Services, Inc. | | 8. CONTRACT OR GRANT NUMBER(s) |
| 9. PERFORMING ORGANIZATION NAME AND ADDRESS Arnold Engineering Development Center/DOFA Air Force Systems Command Arnold AF Station, TN 37389 | | 10. PROGRAM ELEMENT, PROJECT, TASK AREA & WORK UNIT NUMBERS Program Element 65807F |
| 11. CONTROLLING OFFICE NAME AND ADDRESS Arnold Engineering Development Center/DOS Air Force Systems Command Arnold AF Station, TN 37389 | | 12. REPORT DATE October 1981 |
| | | 13. NUMBER OF PAGES 33 |
| 14. MONITORING AGENCY NAME & ADDRESS (if different from Controlling Office) | | 15. SECURITY CLASS. (of this report) UNCLASSIFIED |
| | | 15a. DECLASSIFICATION/DOWNGRADING SCHEDULE N/A |
| 16. DISTRIBUTION STATEMENT (of this Report) Approved for public release; distribution unlimited. | | |
| 17. DISTRIBUTION STATEMENT (of the abstract entered in Block 20, if different from Report) | | |
| 18. SUPPLEMENTARY NOTES Available in Defense Technical Information Center (DTIC). | | |
| 19. KEY WORDS (Continue on reverse side if necessary and identify by block number) vacuum chambers aerodynamic forces Knudsen number gas dynamics rarefied gas dynamics wind tunnels low density pitot tubes Reynolds number | | |
| 20. ABSTRACT (Continue on reverse side if necessary and identify by block number) The cryogenically pumped vacuum chamber has made it possible to generate gas dynamic flows of much lower density than conventional wind tunnels. In the process of calibrating these flows since 1964, pitot tube data have been obtained in a regime that corresponds to very high altitude flight, low Reynolds numbers (<100/cm), or high Knudsen numbers (mean-free-path > 40X pitot diameter). Under these conditions, pitot pressures may be four | | |

UNCLASSIFIED

UNCLASSIFIED

20. ABSTRACT (Continued)

times the inviscid stagnation pressure. Therefore, a substantial correction must be applied to the measured pitot tube data to use it for gas stream calibrations. The available pitot data are correlated in concise form with Reynolds number evaluated behind a normal shock, Re_2 , and total temperature as a parameter. The physical variables are combined in a form of presentation that permits direct determination of stream properties in nozzle or free-jet expansions without the usual successive approximations. The data are presented in a form that permits selection of pitot tube size, transducer range, and applicability of the instrument in specific flow conditions. The use of the pitot tube to survey the rarefied flow of a jet from a rocket motor in a space chamber is discussed. The low density nozzles used in Aerospace Chamber (10V) are probably unique in the low density limit, and the pitot pressure data provide an insight into the gas dynamics of rarefied flows.

PREFACE

The work reported herein was conducted by the Arnold Engineering Development Center (AEDC), Air Force Systems Command (AFSC). The results of the research were obtained by Calspan Field Services, Inc., AEDC Division, operating contractor for Aerospace Flight Dynamics Testing at the AEDC, AFSC, Arnold Air Force Station, Tennessee, under Project Number V41Q-92. The manuscript was submitted for publication on May 19, 1981.

CONTENTS

| | <u>Page</u> |
|---|-------------|
| 1.0 INTRODUCTION | 5 |
| 2.0 EXPERIMENTAL DATA | 5 |
| 2.1 Apparatus | 5 |
| 2.2 Test Conditions | 6 |
| 2.3 Additional Data | 6 |
| 2.4 Analysis of Data | 6 |
| 3.0 APPLICATION OF PITOT DATA TO FLOW | |
| PROPERTIES DETERMINATION | 13 |
| 3.1 Dimensional Analysis | 13 |
| 3.2 Application to Supersonic Nozzle Flow | 14 |
| 3.3 Application to Jets Expanding into Vacuum | 16 |
| 3.4 Examples of Applications | 20 |
| 4.0 CONCLUSIONS | 24 |
| REFERENCES | 25 |

ILLUSTRATIONS

Figure

| | |
|---|----|
| 1. $M = 3$ Nozzle Characteristics — Nitrogen | 7 |
| 2. $M = 6$ Nozzle Characteristics — Nitrogen | 8 |
| 3. Pitot Gage Pressure versus Reynolds and Mach Numbers | 11 |
| 4. Pitot Tube Viscous Effect | 12 |
| 5. Nozzle Flow Pitot Pressure | 15 |
| 6. Pitot Pressure in Free Jet | 19 |

APPENDIX

| | |
|---------------------------------------|----|
| A. Summary of Experimental Data | 27 |
| NOMENCLATURE..... | 32 |

1.0 INTRODUCTION

When the pitot tube is used to make measurements in very rarefied gas streams, there may be a large deviation of the pressure from the ideal inviscid stagnation pressure. This is a low Reynolds number effect common to incompressible, subsonic, and supersonic velocities which requires correction to obtain stream properties from pitot pressure. The low density wind tunnel ($Re/d < 100/cm$) is usually calibrated by use of a pitot tube to determine the Mach number of the stream through isentropic expansion relations which provide density, velocity, and temperature. Because of its simplicity, the pitot tube is attractive for measurements in other flow fields which are not so well defined as the nozzle. The plume formed by a jet exhausting into a vacuum is an important example. The lower limit of nozzle flow corresponds to merging of the wall boundary layers; however, a free jet will continue to expand toward zero density in the absence of wall effects. Therefore, the limit of applicability of the pitot tube requires definition.

In the process of conducting tests with low density nozzles in Aerospace Chamber (10V), a cryogenically pumped altitude chamber, low Reynolds number pitot pressure data have been accumulated. The regime $Re_d < 100$ is of primary interest because it appears that the correlations of Potter and Bailey (Ref. 1) are satisfactory at higher Reynolds number.

2.0 EXPERIMENTAL DATA

2.1 APPARATUS

The approximately 1-m exit diameter LN₂-cooled nozzles designed for Mach numbers of 3 and 6 provided the test stream conditions for supersonic flows of nitrogen. The nozzles exhausted into the chamber, a cryogenically pumped 3-m space simulation chamber. Six pitot tubes were arranged radially about a vertical axis so they could be rotated successively into alignment with the nozzle axis. Each tube could be connected to a 0-1 torr variable capacitance pressure transducer through a sliding valve. The pitot tubes had a 10-deg internal chamfer and a length-to-diameter ratio of 32. The standardized geometry has the advantages of (1) a simple, reproducible form; (2) a large sampling orifice to minimize thermal transpiration effects; and (3) relatively small flow inclination effects compared to other nose shapes.

The following summarizes the pitot tube dimensions.

| <u>Pitot Tube No.</u> | <u>Outside Diameter, cm</u> | <u>Inside Diameter, cm</u> | <u>Length, cm</u> |
|-----------------------|-----------------------------|----------------------------|-------------------|
| 1 | 0.173 | 0.132 | 6.35 |
| 2 | 0.328 | 0.173 | 10.7 |
| 3 | 0.645 | 0.470 | 20 |
| 4 | 0.965 | 0.790 | 30 |
| 5 | 1.286 | 1.117 | 40 |
| 6 | 2.550 | 2.290 | 81 |

The pitot tubes were mounted at the end of a 2.5-cm tube to position them the same distance from the nozzle exit (2 cm). The two smallest tubes failed to produce reliable pressure data because of leakage, outgassing, or excessive fill time for the larger support tube. Thermocouples were spot-welded externally to the pitot tubes 4 to 8 cm from the open ends.

2.2 TEST CONDITIONS

The nozzles can be operated at supply temperatures from 300 to 1,000°K; pressures range from 0.05 to 0.50 torr for the $M = 3$ nozzle and from 0.5 to 3.0 torr for the $M = 6$ nozzle. Figures 1 and 2 show Mach number, Reynolds number, and mean free path operating conditions for nitrogen.

2.3 ADDITIONAL DATA

During several other test programs in the facility, some limited pitot pressure data from small tubes were obtained during nozzle calibrations. A small (0.15- or 0.17-cm-diam) pitot tube was mounted parallel to the 2.5-cm pitot tube used for calibration and moved with it so that the same flow could be sampled in sequence.

As part of a test conducted in the 4-by 6-ft Research Vacuum Chamber, a 0.4-cm sonic orifice was surveyed with a 2.5-cm pitot tube located 50 to 75 cm downstream. The jet that was formed had much lower density than the nozzles and produced the lowest Reynolds numbers observed.

2.4 ANALYSIS OF DATA

The data analysis is based on the general fluid dynamic concept that the ratio of two pressures is the same in a geometrically similar flow field, where similarity depends upon the dimensionless quantities of Mach number, Reynolds number, and a heat-transfer parameter.

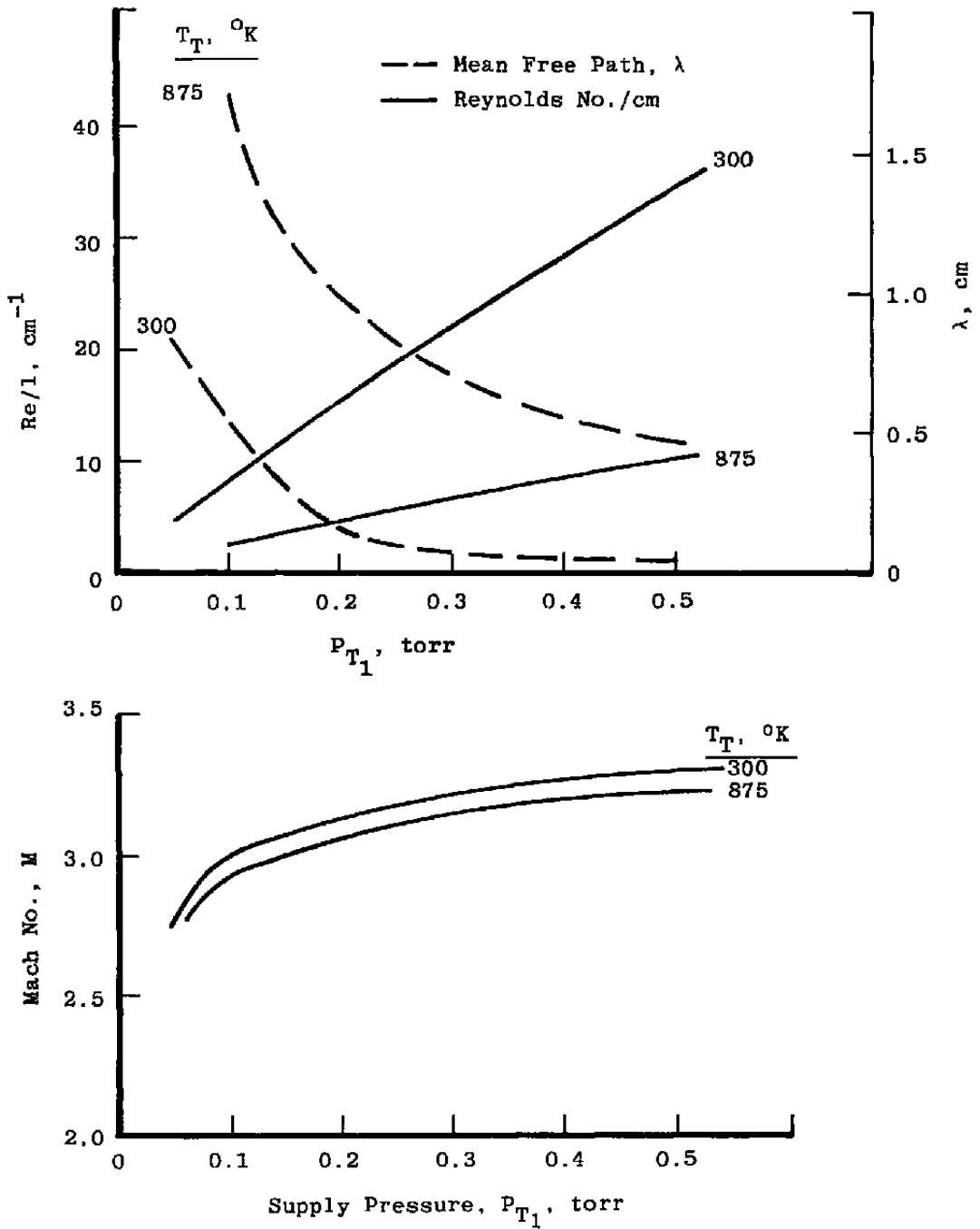


Figure 1. M = 3 nozzle characteristics – nitrogen.

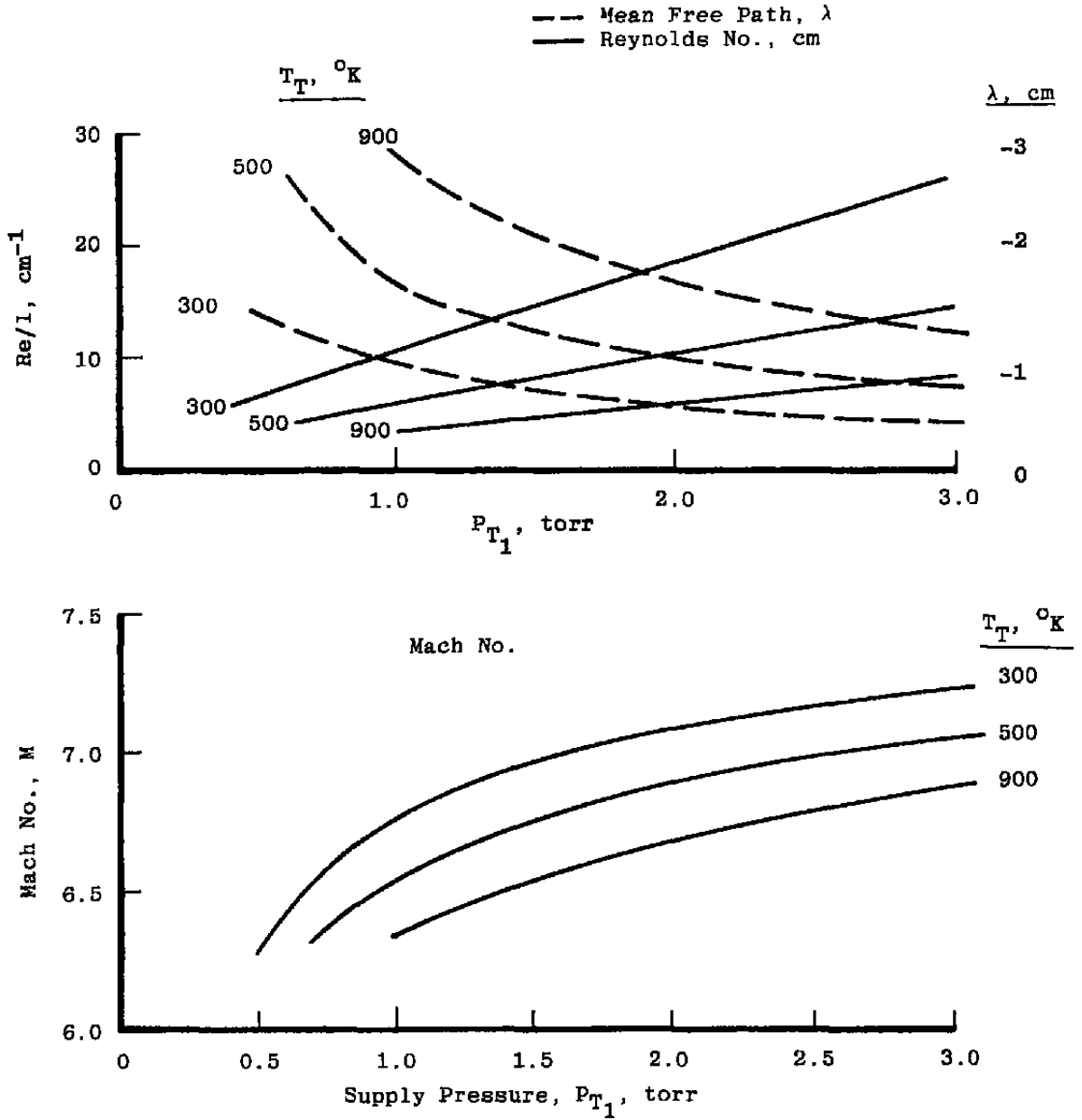


Figure 2. M = 6 nozzle characteristics – nitrogen.

$$P_p/P_{T_2} = f \left(M, Re_d, T_T/T_w \right) \quad (1)$$

The Raleigh stagnation pressure, P_{T_2} , is the pressure at the stagnation point in an inviscid ideal supersonic gas flow. It can be written in terms of the supply pressure, P_{T_1} , for a stream generated by the isentropic expansion through a nozzle as

$$\frac{P_{T_2}}{P_{T_1}} = \left[\frac{(\gamma + 1)M^2}{(\gamma - 1)M^2 + 2} \right]^{\gamma/\gamma-1} \left[\frac{\gamma + 1}{2\gamma M^2 - (\gamma - 1)} \right]^{1/\gamma-1} \quad (2)$$

The pitot pressure, P_p , is conceived as the mean pressure in a small volume just at the entrance of the pitot tube where the temperature, T_p , is practically equal to the stagnation temperature, T_T . The pitot tube wall temperature, T_w , will remain near room temperature for low density (small heat transfer) or short duration flows.

The pitot pressure, P_p , is different from the pitot gage pressure, P_{pG} , because of the thermal transpiration effect (see Ref. 2) which relates the pressure ratio, temperature ratio, and Knudsen number, λ/d_p . The Knudsen number can be defined for the open end of the tube where the pressure is P_p and temperature T_p as

$$Kn_p = \frac{\lambda_p}{d_p} = (\text{const.}) \sqrt{\frac{\pi}{8} \frac{MW}{R_o}} \frac{\mu_p}{\rho_p \sqrt{T_p}} \quad (3)$$

where the viscosity is $\mu = \text{const. } \bar{\rho} \bar{u} \bar{\lambda}$. For the Reynolds number $Re_d = \rho_1 u_1 d_p / \mu_1$ and an exponential viscosity relation $\mu \propto T_1^\omega$,

$$Kn_p = \frac{\text{const.}}{Re_d} M_1 \frac{P_1}{P_p} \left(\frac{T_p}{T_1} \right)^{\omega + 1/2} \quad (4)$$

or since stream (sub 1), supply reservoir (sub T_1), and ideal stagnation conditions (sub T_2), are Mach number relations, the Knudsen number becomes

$$Kn_p = \frac{\text{const.}}{Re_d} f(M) \frac{P_{T_2}}{P_p} \left(\frac{T_p}{T_T} \right)^{\omega + 1/2} \quad (5)$$

where

$$f(M) = M_1 \frac{P_{T_1}}{P_{T_2}} \frac{P_1}{P_{T_1}} \left(\frac{T_T}{T_1} \right)^{\omega + 1/2} \quad (6)$$

The ratio T_p/T_T must be a function of the stream similarity parameters M_1 , Re_d , and T_T/T_w . Therefore, it is evident that the pitot gage pressure P_{PG} , can also be expressed as

$$\frac{P_{PG}}{P_{T_2}} = f(M_1, Re_d, T_T/T_w) \quad (7)$$

This relationship was the basis of the test program in which the $M = 3$ and $M = 6$ nozzles at supply temperatures of 300, 500, and 900°K provided stream conditions over the operating range of supply pressures. The six pitot tubes were rotated in succession into the stream. In general, the Mach number and Reynolds number varied with pressure and temperature. An iterative process was required to separate the effects of M_1 and Re_d from the pitot pressure data at each total temperature. The high Reynolds number starting point for the highest supply pressure was within the range of correlation obtained by Potter and Bailey (Ref. 1) in terms of $Re_2\sqrt{\rho_2/\rho_1}$. The effect of Re_d at constant Mach number and total temperature is observed when the pitot tube diameter is changed. For each nozzle and total temperature, curves similar to Fig. 3 were constructed. This is the functional relationship assumed initially; however, attempts to find a more general correlating parameter showed that the Mach number dependence would be nearly absent when Re_2 was used.

$$Re_2 = \frac{\rho_2 u_2 d_p}{\mu_2} = Re_d \left(\frac{\mu_1}{\mu_2} \right) \quad (8)$$

Figure 4 shows the pitot pressure ratio, P_{PG}/P_{T_2} as a function of Re_2 and total temperature from the faired data discussed in the appendix. Included in these data are results from a sonic orifice exhausting into a vacuum chamber. The 0.15- and 0.17-cm-diam pitot tube data from $M = 3$ and 6 nozzle calibrations are also included, although the accuracy is degraded by the problems of long fill time or outgassing inside the pitot tube system.

The functional relationship between pitot gage pressure, Reynolds number based on conditions behind the bow shock, and the stream stagnation temperature of Fig. 4 provides some insight into the physical phenomena at the stagnation point of a blunt body: (1) there appears to be no tendency for the pressure to approach a free-molecule limit; (2) the stagnation flow field seems to be dominated by viscous effects at low Reynolds number described by the Stokes regime and exhibited in incompressible, continuum flows (see Ref. 4); (3) the effect of total temperature can be interpreted as a reduction of viscosity with temperature as heat is removed from the stagnation region by wall cooling. The effect of decreasing temperature corresponds to increasing Re_2 .

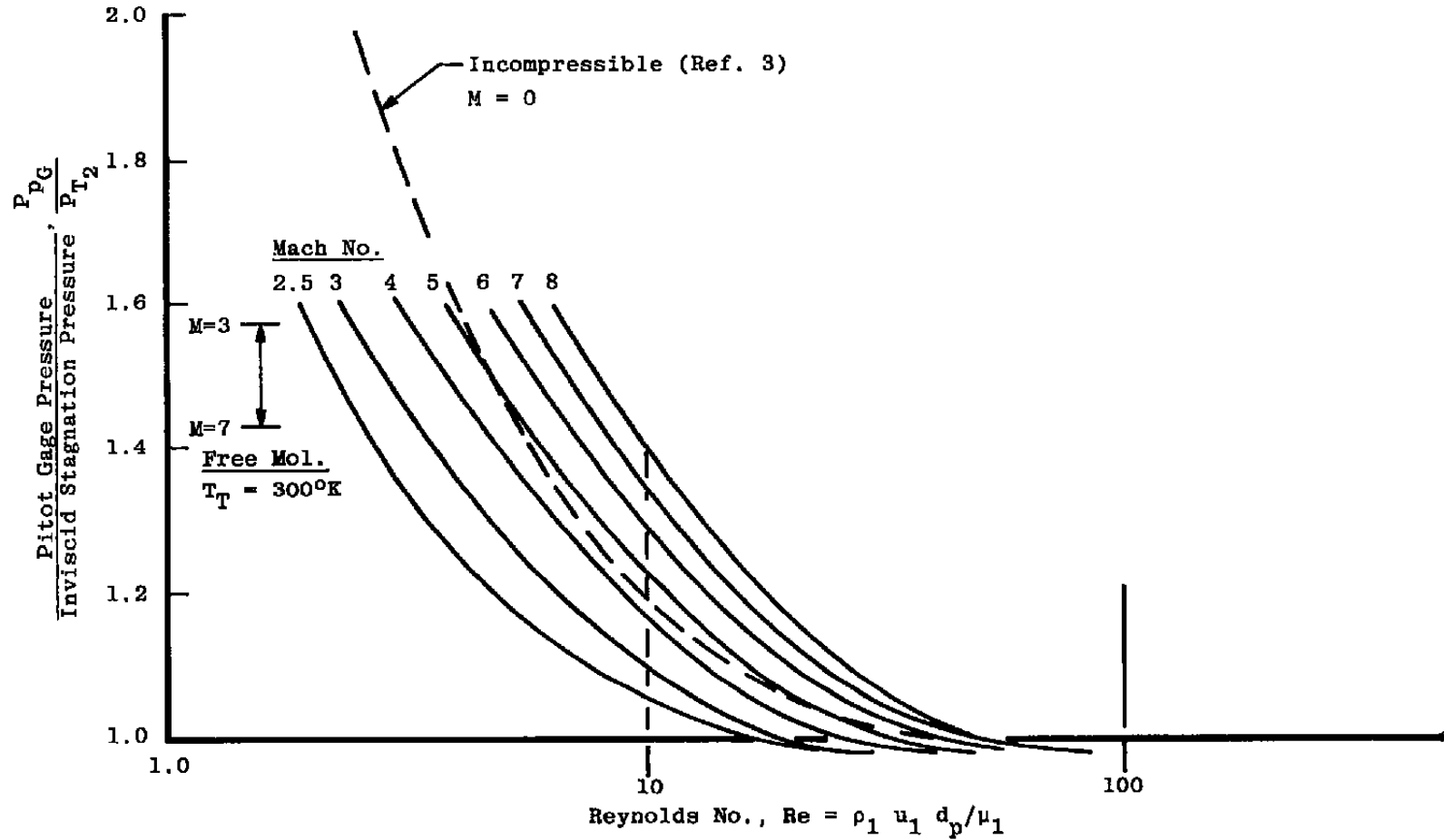


Figure 3. Pitot gage pressure versus Reynolds and Mach numbers.

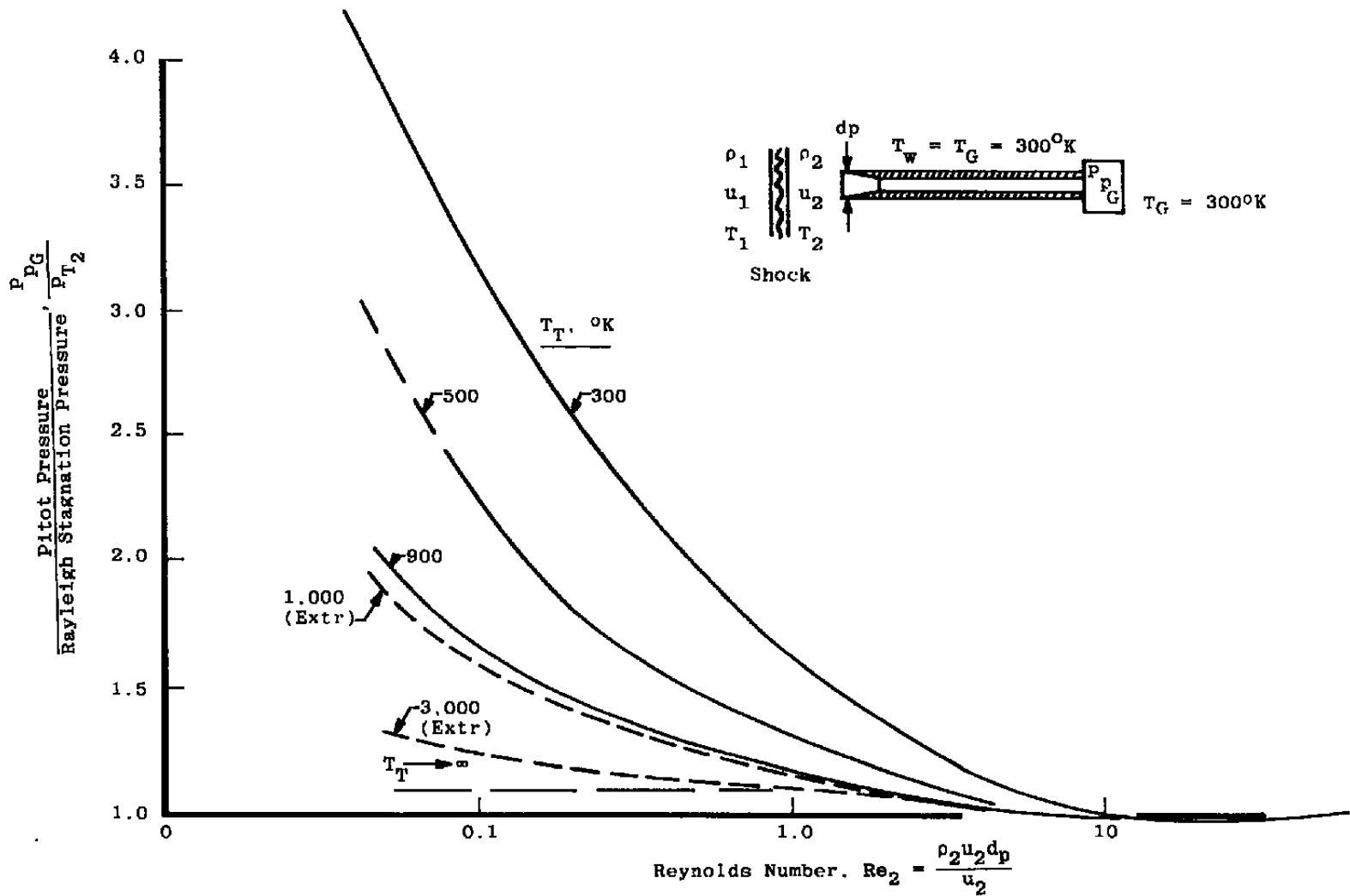


Figure 4. Pitot tube viscous effect.

The perturbation in pitot pressure as the Reynolds number decreases with density is sometimes interpreted as a rarefaction effect (Ref. 4). However, the free-molecule pressure (Ref. 5) shown in Fig. A-3 is evidently not an asymptotic limit for the data. Reference 4 presents pitot data as functions of Knudsen number with free-molecule limits that appear to be approached as the density (or Re) is reduced; however, the data do not extend far enough to establish a leveling off to limiting values. The data of Fig. A-3 distinctly continue beyond the free-molecule limits, and it is evident that such limits are not approached in the experimental regime considered here. The Knudsen number (l/d_p) is as high as 40 at the lowest Reynolds numbers obtained, and there is no evidence that the pitot pressure is tending toward an asymptotic value. One must conclude that the effects observed are viscous in origin; i.e., low Reynolds number effects. These pitot tube results still leave in question the level of rarefaction necessary for a body to be in the free-molecule condition. Certainly the Knudsen number for blunt bodies must be greater than some point in the 10 to 100 range. The experimental difficulties probably preclude measurements in the free-molecule regime.

3.0 APPLICATION OF PITOT DATA TO FLOW PROPERTIES DETERMINATION

3.1 DIMENSIONAL ANALYSIS

The principles of dimensional analysis (see Ref. 6) that permit the rearrangement of functions of dimensionless variables are particularly useful fluid dynamic applications. In the use of pitot tube pressures for the calibration of nozzle flow, the functions can be arranged to avoid the successive approximation method of determination of nozzle Mach number. Figure 4 shows the dimensionless variables.

$$\frac{P_{PG}}{P_{T_2}} = f(Re_2, T_T) \quad (9)$$

and

$$Re_2 = \frac{\rho_2 u_2 d_p}{\mu_2} \quad (10)$$

The known quantities are pitot gage pressure, P_{PG} , pitot tube diameter, d_p , and total temperature. The Mach number can be assumed and the variables ρ , u , μ_2 , and Re_2 can be computed. The process will converge in a few iterations to yield Mach number. However, the variables can be recombined to provide a more convenient form of the data for use; the known quantities appear explicitly so that successive approximations are not necessary. The known variables are supply pressure and temperature, P_{T_1} and T_T , and the pitot gage

pressure, P_{PG} . The unknown is Mach number. The ratio P_{PG}/P_{T_1} can be written as a function of Mach number:

$$\frac{P_{PG}}{P_{T_1}} = \frac{P_{PG}}{P_{T_2}} \left(\frac{P_{T_2}}{P_{T_1}} \right) = \frac{P_{PG}}{P_{T_2}} f_1(M, \gamma) = f(M, \gamma, Re_2, T_T/T_w) \quad (11)$$

and Re_2 is given by

$$Re_2 = \frac{\rho_2 u_2}{\mu_2} \quad d_p = \frac{\rho_1 u_1}{\mu_2} \quad d_p = \frac{\rho_0 u_0}{\mu_0} \quad f_2(M, \gamma) d_p \frac{P_{T_1}}{P_0} \left(\frac{300}{T_T} \right)^{\omega + 1/2} \quad (12)$$

where the subscript (0) refers to 300°K and 1 torr, and ω is the viscosity-temperature exponent.

In Eqs. (11) and (12), the Mach number functions are

$$f_1(M, \gamma) = P_{T_2}/P_{T_1} \quad (\text{See Section 2.4}) \quad (13)$$

$$f_2(M, \gamma) = M \frac{P_1}{P_{T_1}} \left(\frac{T_T}{T_1} \right)^{\omega + 1/2} \left(\frac{T_1}{T_2} \right)^{\omega} \quad (14)$$

3.2 APPLICATION TO SUPERSONIC NOZZLE FLOW

By selecting a value for γ and ω , one can construct a plot like Fig. 5, which has lines of constant Mach number and total temperature. This plot can be entered with the known quantities of supply pressure, P_{T_1} ; total temperature, T_T ; and pitot gage pressure, P_{PG} . The interpolation for Mach number is nearly linear, and it can be readily estimated to about 0.1. If a higher level of accuracy is desired, the Reynolds number can be calculated from Eq. (12),

$$Re_2 = \left(\frac{\rho_0 a_0}{\mu_0 P_0} \right) f_2(M) \left[P_{T_1} d_p \left(\frac{300}{T_T} \right)^{\omega + 1/2} \right] \quad (15)$$

where

$$f_2(M) = M_1 \frac{\rho_1}{\rho_{T_1}} \frac{a_1}{a_T} \left(\frac{T_T}{T_2} \right)^{\omega} \quad (16)$$

and Fig. 4 with

$$M = f\left(\frac{P_{T_2}}{P_{T_1}}\right) \tag{17}$$

In Fig. 5 the reference values are $P_0 = 1$ torr, $T_0 = 300^\circ\text{K}$, $\gamma = 1.4$, and $\omega = 0.76$.

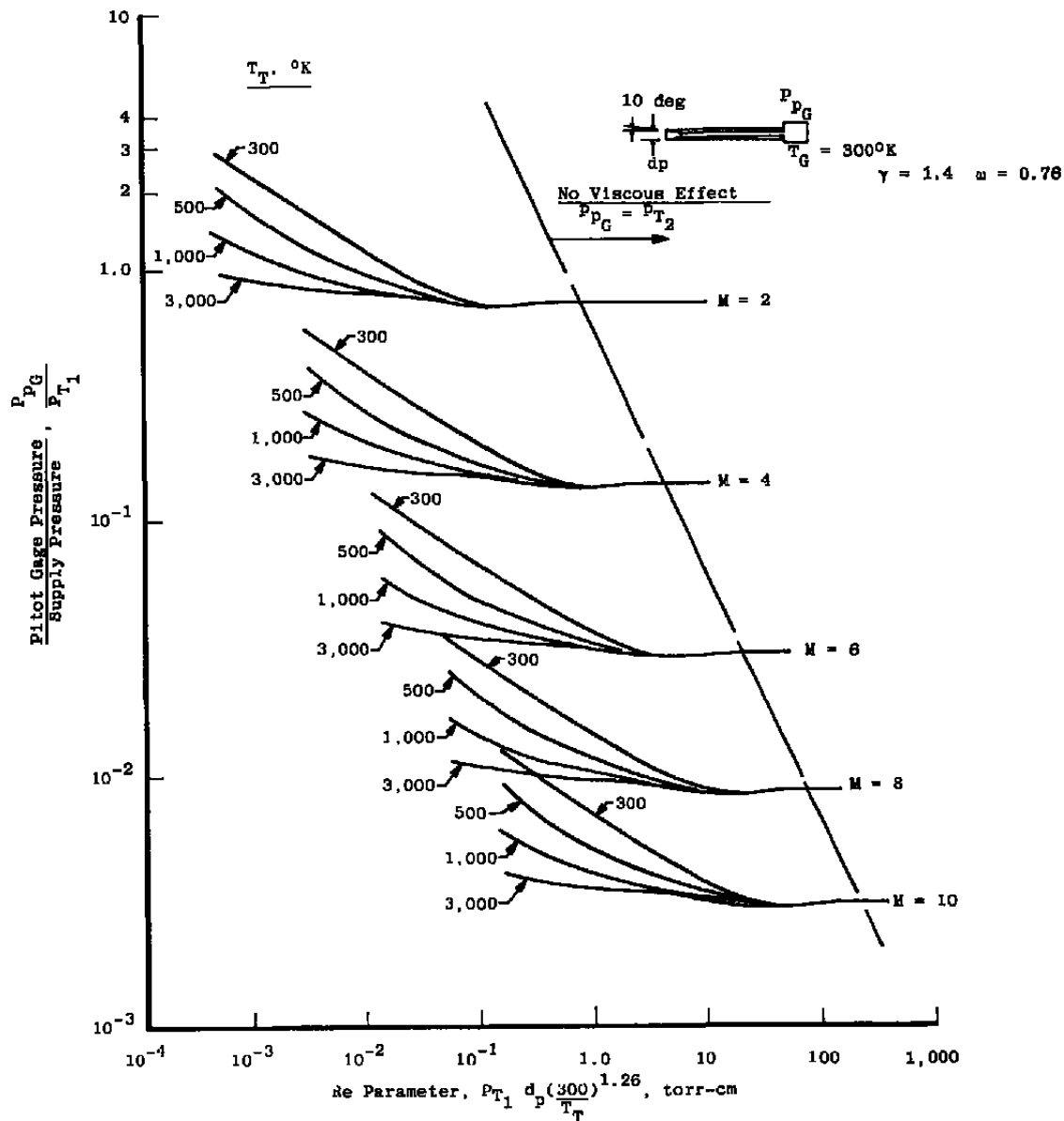


Figure 5. Nozzle flow pitot pressure.

The presentation in Fig. 5 is useful for:

1. Selecting pitot tube size,
2. Selecting pitot pressure gage range,
3. Calibrating supersonic nozzles, and
4. Estimating the conditions for onset of viscous pitot effects.

3.3 APPLICATION TO JETS EXPANDING INTO VACUUM

The flow field of a jet expanding into a vacuum differs from the flow within a nozzle primarily by the much greater rarefaction in the region of interest. In an actual vacuum environment the flow continues to expand indefinitely. The comparison of isentropic (method-of-characteristics) calculations of the flow with experiment (for example, Ref. 7) for molecular beam sources shows that beyond 100 or 200 orifice diameters, the density has an inverse distance-squared variation and the velocity is practically constant. The stream velocity approaches the limit speed determined by the reservoir (total) enthalpy, and the stream temperature tends to approach a constant corresponding to a nonequilibrium state (freezing of one or more modes of molecular energy). The Mach number is no longer a useful flow parameter since it has nearly a constant value depending upon the source temperature, pressure, and size. The local density and velocity are the only physical properties of significance, and they can be combined into the dimensionless quantity

$$\frac{\rho u}{\rho_{T_1} a_{T_1}} = \frac{\dot{m}}{\rho_{T_1} a_{T_1}} \quad (18)$$

where the mass flux, \dot{m} , is normalized by the product of reservoir density and acoustic velocity. Isentropic method-of-characteristics (Ref. 8) calculations of the flow from a nozzle can be reduced to

$$\frac{d\dot{M}/d\theta}{\dot{M}_T} = f(\gamma, \phi, A_e/A^*) \quad (19)$$

where γ is the ratio of specific heats, A_e/A^* is the nozzle area ratio, ϕ is the angle from the axis of the flow field, \dot{M}_T is the total exhaust gas mass flow, and $d\dot{M}/d\theta$ is the mass flow per steradian measured from the nozzle exit. The flow speed is

$$u = u_{L.im} = \sqrt{\frac{2}{\gamma-1}} a_{T_1} = \sqrt{\frac{2\gamma}{\gamma-1}} \sqrt{\frac{R_0 T_T}{(MW)}} \quad (20)$$

and

$$\rho u = \left[\frac{d\dot{M}/d\theta}{\dot{M}_T} \right] \dot{M}_T \frac{1}{R^2} \quad \text{--- mass flux} \quad (21)$$

By using these equations and the Rankine-Hugoniot relations in the limit of large Mach number, one can relate the required flow properties to position in the flow:

1. Reynolds number, Re_2 ,

$$\begin{aligned} Re_2 &= \frac{\rho_2 u_2 d}{\mu_2} = \frac{\rho_1 u_1}{\mu_2} d \\ &= (d/\mu_2) \frac{\dot{M}_T}{R^2} \left[\frac{d\dot{M}/d\theta}{\dot{M}_T} \right] \end{aligned} \quad (22)$$

2. Rayleigh Stagnation Pressure

$$P_{T_2} = f(\gamma) \rho u^2 = f(\gamma) (\rho u) u_{Lim} \quad (23)$$

$$f(\gamma) = \left(\frac{1}{\gamma} \right)^{\gamma/\gamma-1} \left(\frac{\gamma+1}{2} \right)^{\gamma+1/\gamma-1} \quad \begin{array}{cc} \gamma & f(\gamma) \\ 1.2 & 0.96 \\ 1.67 & 0.88 \end{array} \quad (24)$$

$$P_{T_2} = f(\gamma) u_{Lim} \frac{\dot{M}_T}{R^2} \left[\frac{d\dot{M}/d\theta}{\dot{M}_T} \right] \quad (25)$$

3. Stagnation Pressure Ratio, P_{T_2}/P_{T_1} ,

$$P_{T_2} / P_{T_1} = \left[\frac{(\gamma+1) \gamma + 1/\gamma-1 \left(\frac{1}{\sqrt{\gamma-1}} \right)}{(2) \gamma + 3/2 (\gamma-1) \gamma^{1/\gamma-1}} \right] \left(\frac{\dot{m}}{\rho_{T_1} a_T} \right) \quad \begin{array}{cc} \gamma & f(\gamma) \\ 1.2 & 1.62 \\ 1.67 & 2.08 \end{array} \quad (26)$$

4. Dynamic Pressure Ratio, q/P_{T_2}

$$\frac{q}{P_{T_2}} = \frac{1}{2} \frac{\rho u^2}{P_{T_2}} = \frac{(\gamma)^{\gamma/\gamma-1}}{2} \left(\frac{2}{\gamma+1} \right)^{\frac{\gamma+1}{\gamma-1}} \quad \begin{array}{cc} \gamma & f(\gamma) \\ 1.2 & 0.523 \\ 1.67 & 0.567 \end{array} \quad (27)$$

5. Mass Flux Parameter, $\dot{m}/\rho_{T_1} a_{T_1}$,

$$\frac{\dot{m}}{\rho_{T_1} a_{T_1}} = \frac{\dot{M}_T \left[\frac{d\dot{M}/d\theta}{\dot{M}_T} \right]}{\rho_{T_1} a_{T_1} R^2} = \left(\frac{2}{\gamma + 1} \right)^{\frac{\gamma + 1}{\gamma - 1}} \frac{1}{R^2} \left[\frac{d\dot{M}/d\theta}{\dot{M}_T} \right]$$

| | |
|----------|-------------|
| γ | $f(\gamma)$ |
| 1.2 | 0.35 |
| 1.67 | 0.32 |

(28)

Forms (1.) and (2.) have been used in reducing pitot pressure data (Appendix) from sonic orifice flows as the relationship between stream mass flux and the calculated values has been well established for orifices operating at high enough pressures and temperatures to avoid condensation and early nonequilibrium freezing. In these functions, the effect of varying γ (the only characteristic of the gas) is not very important.

It is possible to form parameters by combinations of these dimensionless variables that will simplify the experimental determination of free-jet properties. These are

$$\frac{P_{P_G}}{P_{T_1}} = \frac{P_{P_G}}{P_{T_2}} \frac{P_{T_2}}{P_{T_1}} = f(\text{Re}_2, T_T) \cdot f_1(\gamma) \left(\frac{\dot{m}}{\rho_{T_1} a_{T_1}} \right)$$
(29)

$$* f_1(\gamma) = \frac{1}{f_1(\gamma)} = \frac{(\gamma + 1)^{\frac{\gamma + 1}{\gamma - 1}}}{(2)^{\frac{\gamma + 3}{2(\gamma - 1)}} (\gamma)^{\frac{1}{\gamma - 1}} \sqrt{\gamma - 1}}$$
(30)

$f(\text{Re}_2, T_T)$ - Fig. 4

and

$$\text{Re}_2 = f_2(\gamma) \frac{\rho_{T_1} a_{T_1} d_p}{\mu_T} \left(\frac{\dot{m}}{\rho_{T_1} a_{T_1}} \right)$$
(31)

$$f_2(\gamma) = \frac{\mu_T}{\mu_2} = \left(\frac{T_T}{T_2} \right)^\omega = \left[\frac{(\gamma + 1)^2}{4\gamma} \right]^\omega$$
(32)

Equations (29) and (31), containing known properties of the gas source and pitot pressure, from the coordinates in Fig. 6. The curve parameter, $\dot{m}/\rho_{T_1} a_{T_1}$, is the physically significant property of the free jet, the Mach number being trivial in this case.

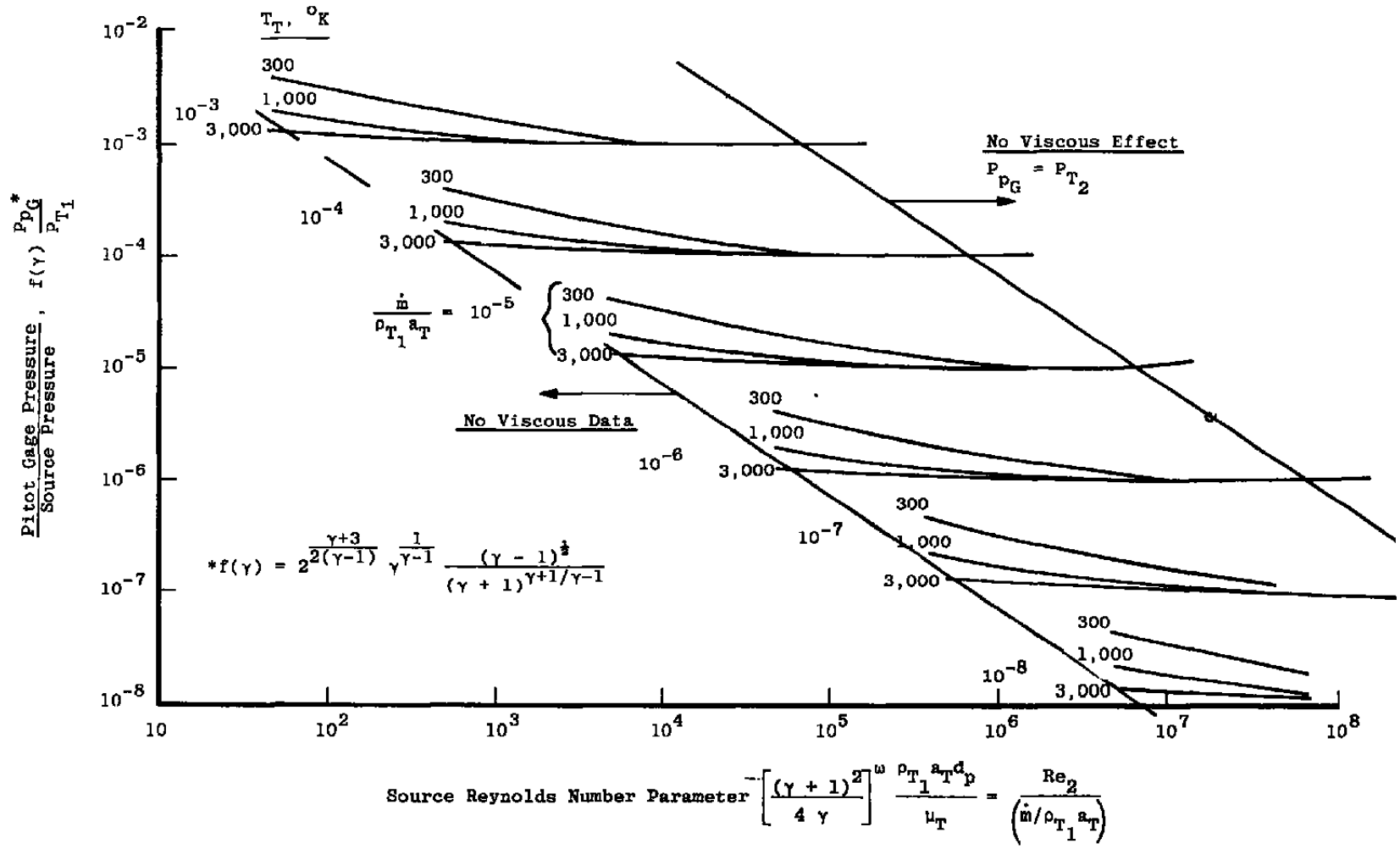


Figure 6. Pitot pressure in free jet.

Two boundaries delineated in Fig. 6 are important in the application of the pitot tube to the jet plume measurement. The right-hand boundary indicates an upper bound of Re , where the viscous effects are negligible. The left boundary is the low limit of pitot data from experiment. Somewhere below the boundary, transition to free-molecular flow occurs, although there is no evidence of it in the available data.

3.4 EXAMPLES OF APPLICATIONS

3.4.1 Supersonic Nozzle Flows

Figure 5 can be used to determine the stream Mach number in supersonic nozzle flow and to select the pitot tube size and pressure transducer range needed to make a measurement in an assumed flow.

To Find the Nozzle Flow Mach Number

The flow in a supersonic nozzle is probed with a 0.5-cm-diam pitot tube. The test conditions are as follows:

| | | |
|-----------------------------------|------------------------|-----------------------------------|
| $P_{PG} = 0.10$ torr | pitot gage pressure | |
| $P_{T1} = 2.0$ torr | nozzle supply pressure | |
| $T_T = 900^\circ\text{K}$ | total temperature | |
| $d_p = 0.5$ cm | pitot tube diameter | |
| Gas N_2 : $\gamma = 1.4$ | $\omega = 0.76$ | $\mu = 1.76 \times 10^{-4}$ poise |

In Fig. 5, $P_{T1} d_p (300/T_T)^{1.26} = 0.25$, $P_{PG}/P_{T1} = 0.050$

$M = 5.4$, Linear Interpolation - First Approximation

A final determination of Mach number can be made if more accuracy is required, by use of Fig. 4. The Reynolds number is

$$Re_2 = \left(\frac{\rho_o^a}{\mu_o} \right) f(M, \gamma) \left[P_{T1} d_p (300/T_T)^{1.26} \right] \quad (33)$$

$$f(M, \gamma) = M \frac{P_1}{P_{T1}} \left(\frac{T_T}{T_1} \right)^{\omega + 1/2} \left(\frac{T_1}{T_2} \right) \quad (34)$$

$$\frac{\rho_o^3}{\mu_o} = 301/\text{cm}$$

$$P_o = 1 \text{ torr}$$

$$T_o = 300^\circ \text{ K}$$

$$Re_2 = 27.8$$

Figure 4 gives $P_{PG}/P_{T_2} = 1.06$

and $P_{T_2}/P_{T_1} = 0.047$

$$M = 5.36$$

as a final value; further approximations will not yield improvement in certainty of the flow Mach number. Since the nozzle flow is isentropic, the density, temperature, and velocity can be calculated immediately.

To Find Pitot Tube Size and Transducer Range

Assume a nozzle flow at a Mach number of 6.0 from a reservoir at 1.0 torr and 500°K:

1. No Viscous Correction

$$M = 6$$

$$P_{T_1} = 1$$

$$T_T = 500^\circ \text{ K}$$

$$P_{T_1} d_p \left(\frac{300}{T_T} \right)^{1.26} = 20$$

$$\frac{P_{PG}}{P_{T_1}} = 0.0295$$

$$d_p = .33 \text{ cm} \quad \text{pitot tube diameter}$$

$$P_{PG} = 0.030 \text{ torr} \quad \text{pitot gage pressure}$$

2. Minimum Diameter Pitot Tube

$$P_{T_1} d_p \left(\frac{300}{T_T} \right)^{1.26} = 1.3 \times 10^{-2}, \quad \frac{P_{PG}}{P_{T_1}} = 0.095$$

$$d_p = 0.024 \text{ cm}$$

$$P_{PG} = 0.095 \text{ torr}$$

which is over three times the inviscid pressure.

3.4.2 Free-Jet Plumes into Vacuum

The selection of a pitot tube size and its transducer range for surveying a jet plume is less certain than for nozzle flow because the flow density can be several orders of magnitude lower. As an example of the use of Fig. 6 to facilitate this process, assume a bipropellant MMH-N₂O₄ motor with the following characteristics:

$$P_{T_1} = P_{Ch} = 8.5 \text{ atm}$$

$$T_T = 3,000^\circ \text{ K}$$

$$\text{Molecular Weight} = 21$$

$$a_T = 1.23 \times 10^5 \text{ cm/sec}$$

$$\gamma = 1.28$$

$$\mu_T = 6.5 \times 10^{-4} \text{ poise}$$

$$A_e/A^* = 20$$

$$\omega = 0.65$$

$$\dot{M}_{Tot} = 150 \text{ gm/sec}$$

$$f(\gamma) = 0.311$$

$$\theta = 40 \text{ deg from axis}$$

$$\text{Dist.} = 3 \text{ m}$$

$$\rho_{T_1} = 7.25 \times 10^{-4} \text{ gm/cm}^3$$

From method-of-characteristics (see Ref. 8) calculations, the plume flow field mass flux is given by

$$\frac{\dot{M}/\theta}{\dot{M}_{Tot}} = f(\gamma, A_e/A^*, \theta) = 0.15/\text{steradian}$$

At a distance of 3 m the mass flux is estimated to be

$$\dot{m} = \rho u = \left[\frac{\dot{M}/\theta}{\dot{M}_T} \right] \frac{\dot{M}_T}{R^2} = 2.5 \times 10^{-4} \text{ gm/cm}^2 \text{ -sec}$$

This is nondimensionalized by the chamber values, $\rho_{T_1} a_T$:

$$\frac{\dot{m}}{\rho_{T_1} a_T} = 2.8 \times 10^{-6}$$

Upon examination of Fig. 6, one finds the upper extreme in Reynolds number gives the pitot tube diameter for no viscous effect

$$\begin{aligned} \frac{Re_2}{\dot{m}/\rho_{T_1} a_{T_1}} &= 2.5 \times 10^7 = \left[\frac{(\gamma + 1)^2}{4\gamma} \right]^\omega \frac{\rho_{T_1} a_{T_1}}{\mu_{T_1}} d_p \\ &= 1.39 \times 10^5 d_p \end{aligned}$$

$$f(\gamma) P_{P_G}/P_{T_1} = 2.6 \times 10^{-6}$$

Therefore, $d_p = 180$ cm for no correction

$$P_{P_G} = 0.055 \text{ torr transducer pressure}$$

The smallest pitot tube for which correction data are available corresponds to the left boundary which shows

$$\frac{Re_2}{\dot{m}/\rho_{T_1} a_{T_1}} = 1.7 \times 10^4 = 1.39 \times 10^5 d_p$$

$$f(\gamma) P_{P_G}/P_{T_1} = 4 \times 10^{-6}$$

Therefore, $d_p = 0.12$ cm smallest diameter

$$P_{P_G} = 0.084 \text{ torr pressure}$$

Between these large limits of pitot tube diameter, compromise must be made among these factors:

1. Spatial resolution improves as d_p decreases.
2. Response time decreases as d_p increases.
3. Uncertainty decreases as d_p increases because $P_{P_G} \rightarrow P_{T_2}$.

4.0 CONCLUSIONS

Pitot pressures have been measured in very low density gas streams of supersonic nozzles and free jets. The low density viscous effects produced pitot pressures over four times the inviscid Rayleigh stagnation pressure. It was found that the ratio of measured pitot pressure to ideal inviscid stagnation pressure correlated with the Reynolds number behind a normal shock wave and a heat-transfer parameter represented by the total temperature when the pitot tube remained near room temperature.

By an appropriate combination of the physical variables, a form of presentation was derived that permits determination of stream properties from pitot pressure without successive approximations. A standard geometry is recommended to minimize the low Reynolds number and angle of flow effects. The simple geometry is a 10-deg internally chamfered tube about 30 diameters long.

The boundaries shown in Figs. 5 and 6 permit the determination of pitot tube size and pressure transducer range required to make successful measurements in wind tunnel nozzles or free-jet plume flow fields. The limit of applicability of the pitot tube as a measuring instrument for very low density flows is also indicated by the boundaries. In the case of nozzle flow, the convergence of the wall boundary layer will cause merged flow before the limit of pitot tube applicability. However, the free jet may expand to a density where pitot data are unavailable and the measurements are uncertain.

REFERENCES

1. Potter, J. L. and Bailey, A. B. "Pressures in the Stagnation Regions of Blunt Bodies in the Viscous-Layer to Merged-Layer Regimes of Rarefied Flow." AEDC-TDR-63-168 (AD416004), September 1963. See also *AIAA Journal* Technical Note, April 1964.
2. Arney, G. D. and Bailey, A. B. "Addendum to an Investigation of the Equilibrium Pressure Along Unequally Heated Tubes." AEDC-TDR-62-188 (AD286166), October 1962. See also J. AIAA Technical Note, December 1963.
3. Hurd, C. W., Cheskey, K. P. and Shapiro, A. H. "Influence of Viscous Effects on Impact Tubes." *Journal of Applied Mechanics*, Vol. 20, No. 2, June 1953, pp. 253-256.
4. Enkenhus, K. R. "Pressure Probes at Very Low Density." University of Toronto Institute of Aerophysics Report No. 43, OSR-TN-57-237 (AD126534), January 1957.
5. Schaaf, S. A. and Chambre, P. L. *Vol. III High Speed Aerodynamics and Jet Propulsion*. Princeton University Press, Princeton, New Jersey, 1958.
6. van Driest, E. R. "On Dimensional Analysis and the Presentation of Data in Fluid Flow Problems." *Journal of Applied Mechanics*, Vol. 13, No. 1, March 1946, pp. A-34-A-40.
7. Ashkenas, H. and Sherman, F. S. "The Structure and Utilization of Supersonic Free Jets in Low Density Wind Tunnels" in *Proceedings of the Fourth International Symposium on Rarefied Gas Dynamics*, Vol. II. Edited by J. H. deLeeuw, Academic Press, New York, 1966, pp. 84-105.
8. Dawbarn, R., Arnold, F., and Stephenson, W. B., et al. "Development of an Integrated Cryogenic Pumping System for Rocket Plume Studies." AEDC-TR-71-19 (AD880649), February 1971.
9. Lefkowitz, B. and Knuth, E. L. "A Study of Rotational Relaxation in a Low-Density Hypersonic Free-Jet by Means of Impact-Pressure Measurements" in *Proceedings of the Sixth International Symposium on Rarefied Gas Dynamics*, Vol. II. Edited by Leon Trilling and Harold Y. Wachman, Academic Press, New York, 1969, pp. 1421-1438.

APPENDIX A

SUMMARY OF EXPERIMENTAL DATA

The systematic data from the 0.6- to 2.6-cm-diam pitot tubes are shown in Fig. A-1 reduced to pitot gage pressure as a function of Reynolds number behind a normal shock and total temperature. The temperature should be considered a heat-transfer parameter, which would more properly be written T_T/T_w (Total Temperature/Pitot Tube Temperature). The gage temperature in these tests was maintained near room temperature by a thermostatically controlled heater. The Mach numbers for the two nozzles cover a range from 2.7 to about 7.0, and the independence of the pressure ratio is evident in the figure.

Figure A-2 summarizes some pitot pressure data in a free-jet expansion from a 3.8-mm sonic orifice into a cryogenically pumped chamber. Reference 7 gives results of method-of-characteristics calculations of the sonic jet flow field in the form of flow density variation

$$\frac{\rho}{\rho_{T_1}} = \frac{\text{const.}}{r^2} \quad \text{along the axis} \quad (\text{A-1})$$

where the constant depends upon the ratio of specific heats, γ , and orifice area.

Since the flow is nearly fully expanded, the velocity is given by the total enthalpy to a good approximation: $u_{Lim} = \sqrt{2/\lambda - 1} a_T$. The Rayleigh stagnation pressure for an inviscid isentropic gas flow, P_{T_2} , approaches the limiting value

$$P_{T_2} = f(\gamma) \rho u_{Lim}^2 \quad (\text{A-2})$$

where

$$f(\gamma) = (1/\gamma)^{\gamma/\gamma-1} \left(\frac{\gamma+1}{2} \right)^{\gamma+1/\gamma-1} \quad (\text{A-3})$$

In Fig. A-2 the ratio of the measured pitot pressure to the Rayleigh stagnation pressure is shown as a function of Reynolds number based on conditions behind the normal shock where temperature is practically the stagnation temperature, i.e.,

$$Re_2 = \frac{(\rho_2 u_2) dp}{\mu_T} \approx \frac{(\rho u_{Lim}) dp}{\mu_T} \quad (\text{A-4})$$

These data were obtained for a room temperature source and include similar data from Ref. 9 for an externally chamfered pitot tube. The Reynolds numbers were based on the pitot tube nose diameter and the curve compares well with the AEDC sonic orifice results.

Figure A-3 summarizes the AEDC data obtained in the supersonic nozzles and the sonic orifice. The experimental scatter is larger for the lower Reynolds numbers, but the trends for $Re_2 \leq 1$ appear consistent with the more reliable data of Fig. A-1. Incompressible pitot pressures (measured by cylindrical tubes in water and oil--see Ref. 3) are included to demonstrate that the low Reynolds number rise in pitot pressure is not logically a rarefaction effect, but is associated with the domination of viscous over dynamic stresses. The Stokes or Oseen regimes are characteristic of this form of behavior. There is no evidence in the present experimental data ($Re_2 \cong 0.1$) for an approach to a free molecule limit in pitot pressure.

The temperature of the pitot tube was measured 4 to 8 cm from the nose by copper-constantan thermocouples, and the following table lists typical temperatures during the experiments.

| <u>T_T, °K</u> | <u>P_T, torr</u> | <u>T_P, °K</u> | <u>Nozzle</u> |
|--------------------------|----------------------------|--------------------------|---------------|
| 300 | 0.05 - 0.50 | 270 - 290 | M = 3 |
| 900 | 0.05 - 0.50 | 280 - 340 | M = 3 |
| 500 | 0.50 - 3.0 | 270 - 300 | M = 6 |
| 900 | 0.50 - 3.0 | 280 - 326 | M = 6 |

The cold chamber walls, low heat transfer in a vacuum, and the small convective heat transfer in low density flow combine to limit the pitot tube temperatures about room temperature.

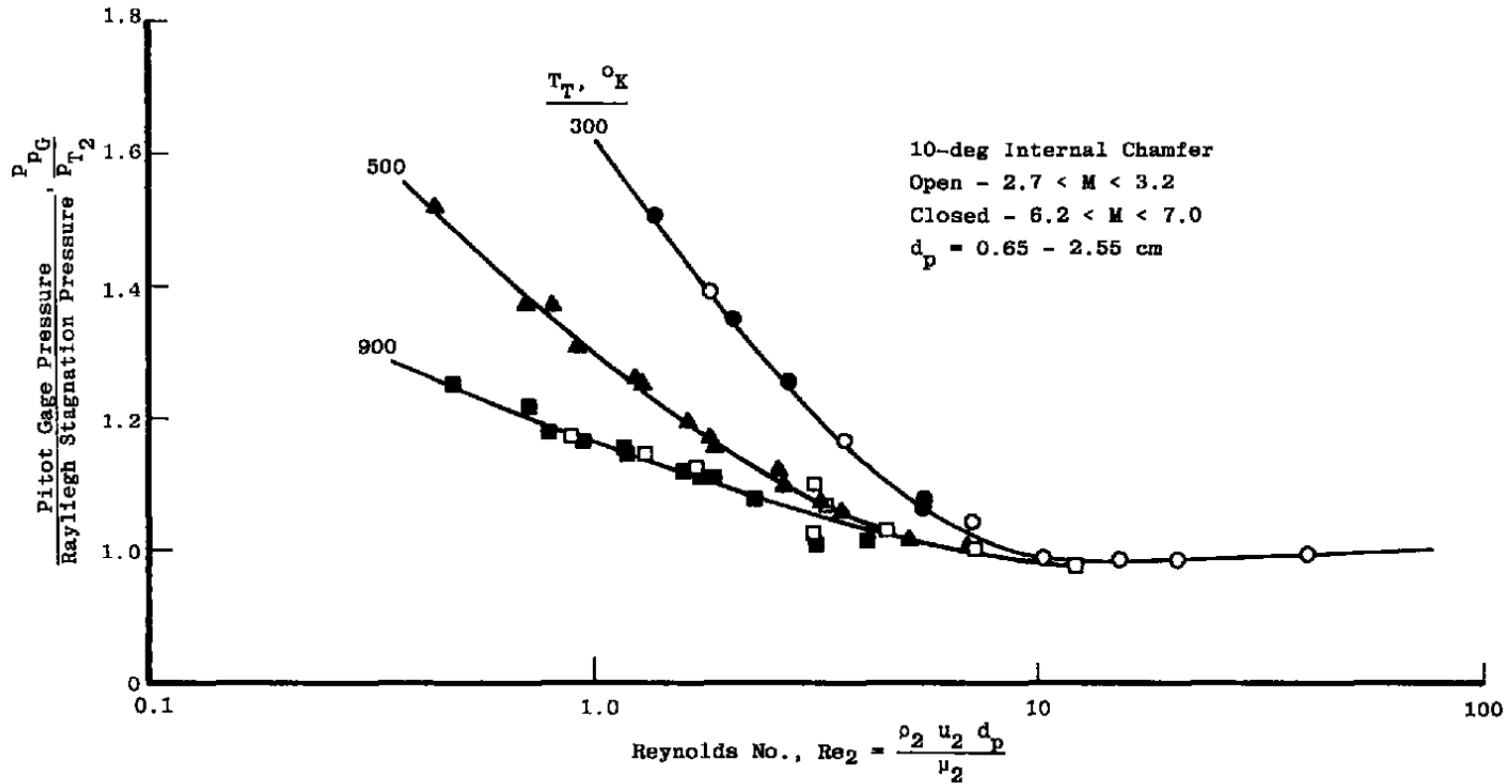


Figure A-1. Pitot tube data-supersonic nozzles, September 1967 (N_2).

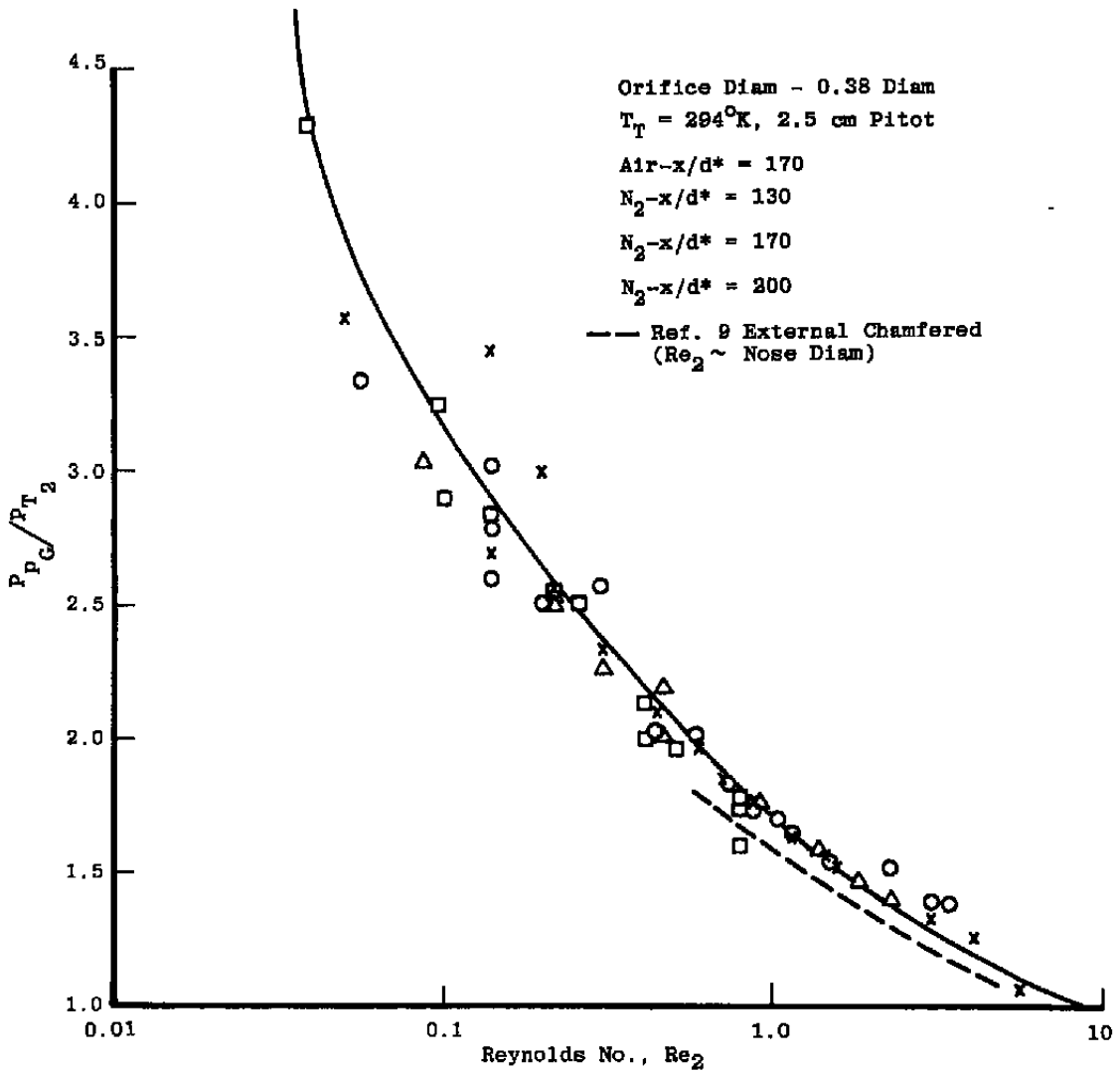


Figure A-2. Pitot pressure in sonic orifice jet

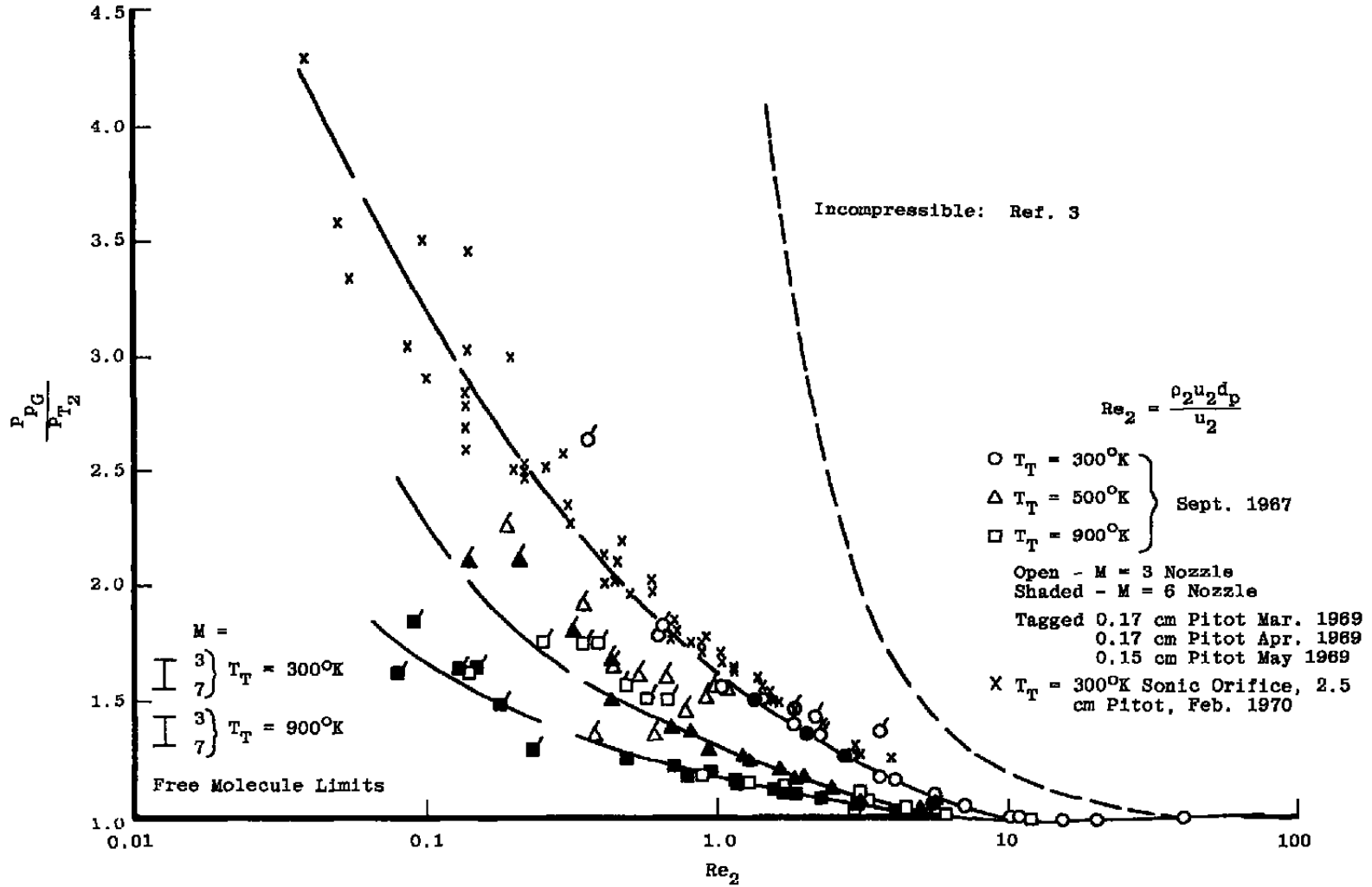


Figure A-3. Pitot pressure summary.

NOMENCLATURE

| | |
|-------------|---|
| A_e | Cross section area of nozzle exit |
| A^* | Nozzle throat area |
| a | Acoustic speed |
| d | Diameter of pitot tube |
| Kn | Knudsen number, (λ/d) |
| \dot{M} | Mach number, (u/a) |
| \dot{M} | Mass flow rate |
| MW | Molecular weight |
| \dot{m} | Mass flux, (ρu) |
| P_p | Pitot pressure |
| P_{p0} | Pitot gage pressure |
| P_{T1} | Stagnation pressure ahead of normal shock |
| P_{T2} | Stagnation pressure behind normal shock (inviscid) |
| R | Radial distance |
| R_o | Universal gas constant |
| Re_2 | Reynolds number behind normal shock, $(\rho_2 u_2 d_p / \mu_2)$ |
| Re_d | Reynolds number, $(\rho_1 u_1 d_p / \mu_1)$ |
| $T_p = T_w$ | Pitot tube wall temperature |
| T_T | Stagnation temperature |

| | |
|-----------|--|
| u | Flow velocity |
| \bar{u} | Random mean velocity |
| γ | Ratio of specific heats, (C_p/C_v) |
| θ | Plume streamtube solid angle |
| λ | Mean free path |
| μ | Coefficient of viscosity |
| ρ | Density |
| ϕ | Angle from nozzle axis |
| ω | Viscosity-temperature exponent |

SUBSCRIPTS

| | |
|-----|---|
| o | Reference condition, (1 torr and 300°K) |
| 1 | Ahead of normal shock |
| 2 | Behind normal shock |
| p | Pitot tube |
| T | Stagnation point |